Analysis of AMPA staining after blocking of NMDA receptors

Max Ligthart, BMT bachelorassignment
Clinical Neurophysiology department, (CNPH), University of Twente
Supervisors: Dr.Ir. J. Le Feber and M. Lamberti
July 4, 2024

Previous research showed that blockage of NMDA receptors led to an unexpected increase of electrical stimulation responsiveness in rat cortical cell cultures in-vitro at six hours after APV addition. Due to expected decrease, the experiment was investigated and repeated again using immunostaining. Fluorescent images of neuron processes at zero and six hours after APV addition were analysed to determine if the total amount of AMPA receptors changed and whether the amount of synapses increased. Analysis included colour intensity of processes and puncta. A difference in the mean colour intensity between processes was found, which suggests that more AMPA receptors are present after NMDA blocking.

Keywords: AMPA, NMDA , APV, STDP, IHC, Neurons.

1 Introduction

On a normal day, we greet familiar faces, go to work and make dinner. This would all be impossible without memory. Memory in our brain is an intricate system of connected neurons that through exchanges of neurotransmitters remember certain events.

Neurons are cells that convey information through electric pulses[1]. They are connected via synapses, having pre- and postsynaptic neurons. Presynaptic neurons send neurotransmitters through the synaptic cleft to the postsynaptic neurons that might cause a postsynaptic action potential[2]. This potential can create a chain reaction to other neurons further on in the network to exchange information.

Postsynaptic neurons receive neurotransmitters through receptors, such as NMDA (N-methyl-D-aspartate) and AMPA (α-amino-3-hydroxy-5-methyl-4-isoxazolepropionic acid) receptors. Glutamate, the most common excitatory neurotransmitter in the cortex, binds to these receptors, which causes their ion channel to open, letting Na^{2+} or Ca^{2+} pass to the cytoplasm[3,4]. For NMDA receptors, this passage is usually blocked by magnesium ions. These ions can be forced out of the passage through depolarisation of the cell, for example by AMPA receptor activation[4,5]. A visual representation can be seen in Figure 1.

Through aforementioned mechanism, the NMDA receptor acts as an action potential 'booster', which causes further depolarisation of the cell to possibly overcome the threshold, generating an action potential to continue or start the chain reaction.

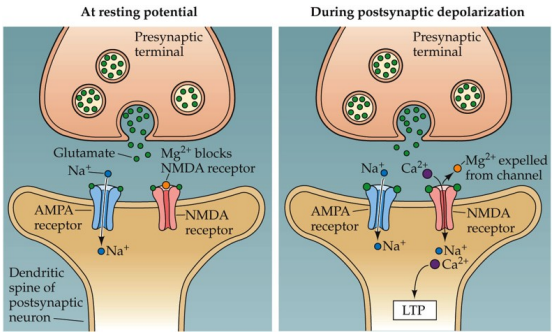

Figure 1: Opening of an NMDA receptor: a magnesium ion blocks the passage of positive sodium ions. An AMPA receptor does let them through, causing a depolarisation in the postsynaptic neuron, which releases the Mg^{2+} ion. This now lets Ca^{2+} and Na^{2+} pass through the NMDA receptor as well.[6]

Our brain undergoes physical changes to learn or form memories, utilising so-called synaptic plasticity. This plasticity is neurons strengthening or weakening their synaptic connections with neighbouring neurons. Spike-timing dependent plasticity (STDP) is an important plasticity mechanism that has been associated with memory formation and consolidation. Depending on the depolarisation timing between the pre- and postsynaptic neuron, the synaptic connection may be strengthened or weakened. If the presynaptic neuron fires before the postsynaptic neuron, it is known as long term potentiation (LTP), with the other way around leading to long term depression (LTD)[7]. STDP is, among other factors, initiated by the extra calcium ions provided by NMDA receptors[8,9].

In a previous article by M. Lamberti et al., the activity of in-vitro networks of rat cortical cells was measured to study the mechanisms of NMDA receptors in memory. It was observed that NMDA receptors are essential for the formation of memory traces[10]. Experiments were done with blockage of NMDA receptors using its antagonist APV, also known as AP5 or DL-2-amino-5-phosphonopentanoic acid. It was assumed that the excitability would decline as NMDA-receptors were turned off. However, the results showed an increase in electrical stimulation response in the first six hours, which declined afterwards, as can be seen in Figure 2. This initial increase was hypothesised to reflect activity homeostasis, which could increase the number of AMPA receptors, aiming to compensate for the blocked NMDA receptor[10]. AMPA receptors could compensate by increasing in amount for normal synapses, or unsilence silent synapses. Silent synapses only have NMDA receptors, thus unsilencing them with the presence of new AMPA receptors[11].

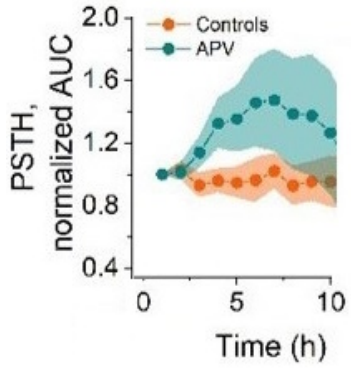

Figure 2: Electrical stimulation response in a previous article by M. Lamberti et al. A peak can be seen at around 6 hours for APV.[10]

In this paper possible explanations will be looked into by answering the following research question: 'Does the AMPA receptor quantity increase after blockage of NMDA receptors with APV?'. This will be achieved by staining AMPA receptors in rat cells through immunohistochemistry and analysis of microscope images to determine if the total amount of AMPA receptors changes and if the amount of synapses increases. The results can provide more insights into the inner workings of the brain.

2 Materials and methods

2.1 Experiments

Cell cultures The used cell cultures were obtained from brain cortices of newborn Wistar rats. All surgical and experimental procedures complied with Dutch and European laws and guidelines (AVD110002016802). The cultures were kept in culture for at least two weeks, during which the medium was changed twice a week. The medium consisted of Neurobasal A medium (ThermoFisher, A2477501), B27 (ThermoFisher, 17504044), D-glucose (Sigma-Aldrich, G7021), Pen/strep (ThermoFisher, 10378016), nerve growth factor (Sigma-Aldrich, n6009) and vitamin C (Sigma-Aldrich, A4544). Fixation took place a day after the medium was changed.

Experimental design The same experiment was done three times, all having an APV and control group. For the control no other solutions were added as replacement of APV. The groups were further divided into zero hours and six hours after APV addition. In total, eight coverslips per condition were made. An overview of the conditions can be seen in Figure 3. *Fixation* In the APV wells, 0.5 µL of APV was pipetted into the medium. For the zero hours group, the medium with APV was aspirated, after which the cells were washed using 0.5 ml phosphate-buffered saline (PBS, ThermoFisher, 70011044) and fixed in 0.5 ml of a 10% solution of paraformaldehyde (PFA, PanReac, 141451) in PBS for ten minutes. For the six hours group, the control and APV group were first put into the incubator for six hours after the APV group had APV addition. Afterwards, they were also washed with PBS. The six hours group was also fixed in 0.5 ml of a solution of 10% PFA in PBS for ten minutes. Finally, after fixation all cultures were washed twice in PBS and stored in the refrigerator at 4° C with PBS.

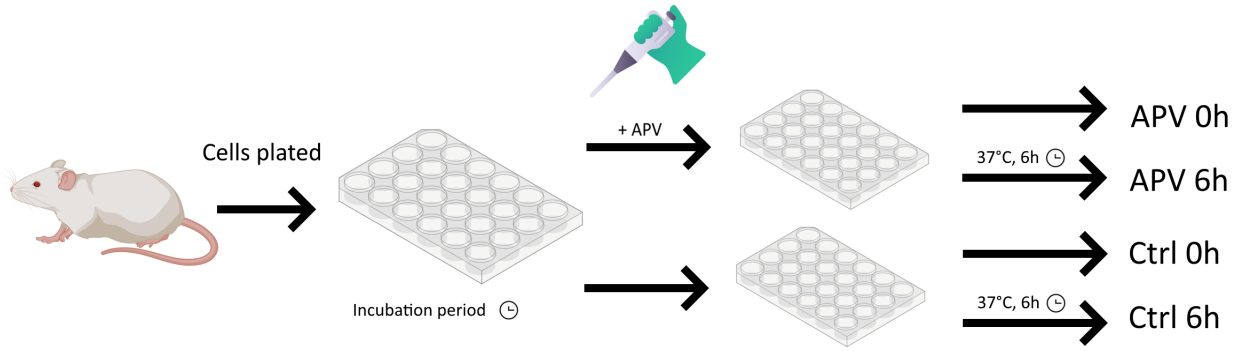

Figure 3: Overview of all different conditions. Incubation time was 26 days for experiment 1 and 2, 19 days for experiment 3. Medium was changed twice a week during the incubation period. A day after medium change, APV was added and fixation took place. All groups were fixated after the final step.[12–14]

Staining The day after, every well was washed again with PBS, following the addition of PBS with 2% bovine serum albumin (Sigma-Aldrich, A1595), as a blocking buffer. After one hour, the blocking buffer was aspirated. A solution with the blocking buffer and two primary antibodies was made: rabbit anti-GLUR2 for AMPA staining (Bioss, bs-10042R, 1 mg/ml, diluted 1:100) and mouse anti-MAP2 to stain neurons (Sigma-Aldrich, M4403, 4-10 mg/ml, diluted 1:200). The next day, 1 ml of PBS was used to wash the coverslips. A new solution was made with the blocking buffer and secondary antibodies, anti-rabbit for AMPA (ThermoFisher, A-11036, 2 mg/ml) and anti-mouse for MAP2 (ThermoFisher, A-11029, 2mg/ml). Both antibodies were diluted to 1:1000. These coverslips were then also stained for cell nuclei with the blocking buffer and 1:1000 DAPI (Sigma-Aldrich, 32670, 300 µM). The coverslips were moved to a microscope slide plate, with Mowiol (Polysciences inc., 25213-24-5). A slide tray with the prepared coverslips was kept in the dark overnight. Finally, the tray was stored in the refrigerator at 4° C.

2.2 Microscopic imaging

All images were obtained using a fluorescence microscope at 60x magnification (Nikon eclipse 50i clinical microscope). For each coverslip five different locations were imaged three times, each with a different staining: AMPA (red), MAP2 (green) and DAPI (blue). An overlay of all these stainings together can be seen in Figure 4. This resulted in fifteen images per coverslip all in *.tif*-format. Since each condition had eight different coverslips and the script uses only the AMPA staining, forty different images per condition were used for analysis. The image locations were chosen using DAPI such that two to ten nuclei were visible per location. If the resulting location had too much red staining for the script, a different location was chosen. If too many locations were not suitable, a representative area was selected based on the AMPA staining.

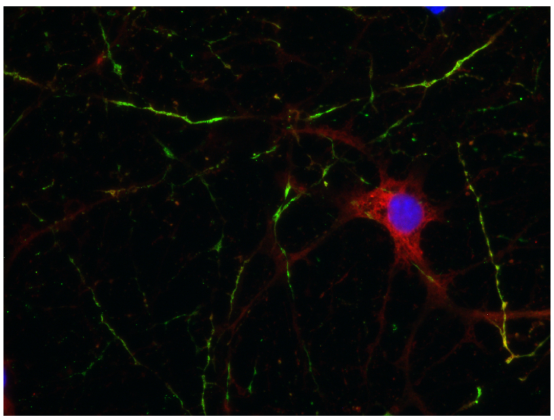

Figure 4: An image of all immunostainings together. AMPA can be seen in red, MAP2 in green and DAPI in blue.

2.3 Data analysis/script

All photos were analysed using a MATLAB script made for this paper. The aim of the script was to gain two main readouts from the microscopic pictures: the average intensity of red fluorescence in neuronal processes, using the Red Green Blue (RGB) scale, as well as the number of puncta per unit of area in these processes. As a first step, the average red intensity was calculated for the entire image. Then, the average intensity of processes was used to estimate the total number of AMPA receptors, while the puncta were used to estimate new synapses with AMPA receptors. Figure 5A shows an example of an unedited image.

The script first isolates all the red values. A threshold was set at 10% of the highest red value to detect all red fluorescent areas. Through trial and error, 10% was found to be the best general fit for all images. A binary matrix, called $Matrix\_red$, is made with all the boolean data if that pixel is above the threshold, this can be seen in Figure 5B. All selected areas are shown in blue, with the original image as a background. Erosion was applied to separate the processes from $Matrix\_red$, leaving only the large 'clouds', see Figure 5C. Moreover, the remaining areas are enlarged by a function to mimic their pre-eroding or original size, see Figure 5D. The result is used to eliminate these areas from $Matrix\_red$, resulting in Figure 5E, in the script referred to as $Processes\_output$. These are the selected processes the script will use.

To extract the puncta, an average red value is calculated from each of the selected parts in Figure 5E. When looking at the puncta in the processes, it was noticeable that the puncta were slightly brighter than most parts of the processes. This also results in being slightly above the average of a local area, which can be used as a criteria. A local area is defined as an area consisting of only directly connected pixels. Furthermore, every value that exceeds this local average with 5%, 10% or 15% is kept in matrices $Puncta5$, $Puncta10$ and $Puncta15$ respectively, these are the found puncta. These results can be seen in Figure 5F-H. Finally, large areas, mostly found around cell bodies, are removed, with the aim of keeping the puncta in the processes.

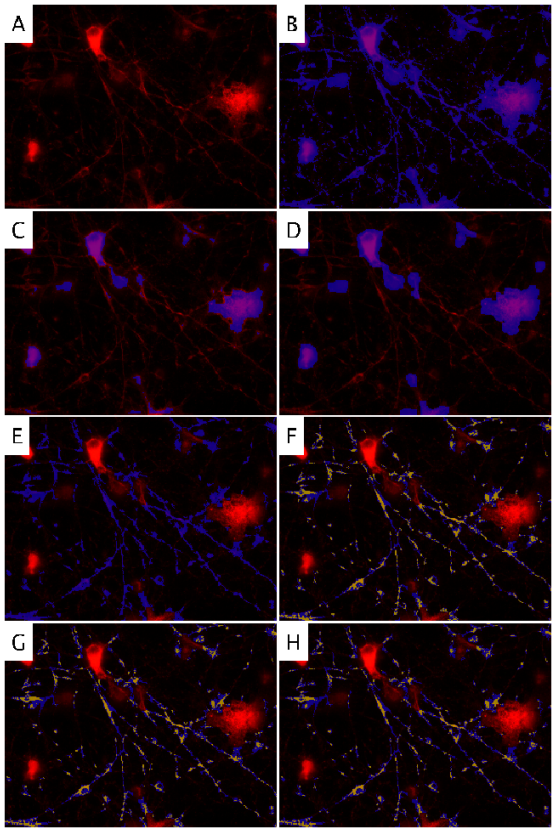

Figure 5: An example of the step-by-step analysis done by MATLAB. A: original image with red immunostaining of AMPA at 60x magnification. All other images have an overlay of this image. B: all red values above 10% of the maximum red value, shown in blue. C: parts remaining after eroding B. D: parts after enlarging C (see text). E: resulting parts after excluding D from B. F-G: blue is the selected processes of E, with yellow being pixels above the set thresholds of the local average of 5% (F), 10% (G) and 15% (H).

With all these matrices computed, the total amount of pixels in each puncta matrix is divided by the detected pixels in $Processes\_output$, resulting in a percentage per photo. This is the amount of found puncta pixels per process pixel. The average amount of red in the selected processes is also calculated with the values from Figure 5E. Each image was put through the script with the same parameters.

2.4 Statistical analysis

Normality was checked using the Shapiro-Wilk test, which showed that some samples were normally distributed, while others were not. Thus, the non parameteric Wilcoxon rank sum or Mann-Whitney U test was used for comparing all datasets in the results. P-values lower than 0.05 were considered to be significant. Also, since all data is assumed to be not normally distributed, the median and IQR is used instead of the mean and standard deviation. Apart from a statistical comparison between conditions, the control group was also analysed between experiment batches. This was done to see if there was a significant distinction between the controls for the batches.

3 Results

Firstly, the mean red intensity was calculated for each entire image. The results can be seen in Figure 6. The spread of values was relatively large with many outliers. The data obtained was non-representative and inaccurate, since it largely depends on how many cell bodies were in the image. The more cell bodies, the higher the mean red intensity. To improve analysis, only the processes were further analysed and cell bodies were excluded. Examples of images can be seen in Figure 7 that also includes comparison between calculated intensity values.

For mean red values of processes, no significant difference was found between ctrl 6h and ctrl 0h ($p = 0.1029$), but there was a difference found between APV 0h and APV 6h ($p = 0.0021$), which can be seen in Figure 8. The spread is much smaller and has less outliers than in Figure 6.

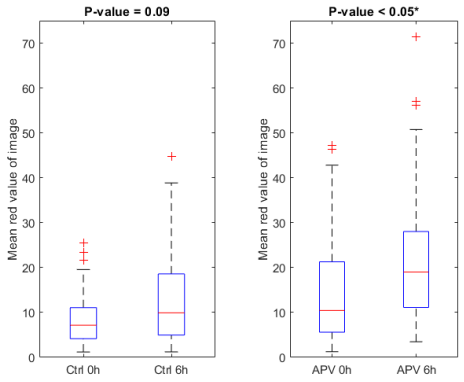

Figure 6: The mean red intensity of entire images without any processing (for each condition N = 40). The controls did not differ from each other (p = 0.0894), while the APV groups did (p = 0.0212). However, this data relied too heavily on how many cell bodies were present. Thus, for further analysis only processes were analysed.

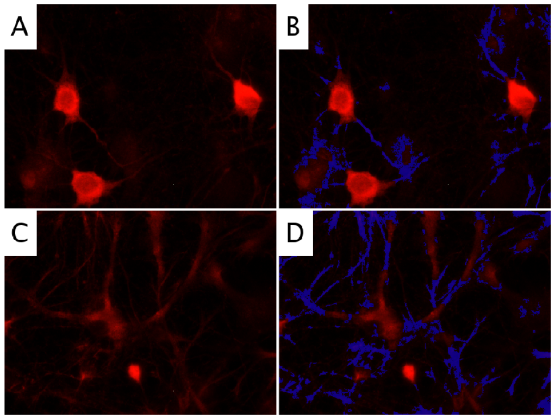

Mean red value of	Entire image	Processes
Image A-B	21.69	33.63
Image C-D	19.32	36.39

Figure 7: Obtained AMPA fluorescence images using immunostaining with their respected outputs of the script. On the left the original image at 60x magnification, on the right with overlaying selected processes in blue. A-B: AMPA image in experiment 2 from the APV 0h group. C-D: AMPA image in experiment 2 from the APV 6h group. When looking at the entire image, image A has a higher red value, while for the analysed processes image B has the higher value.

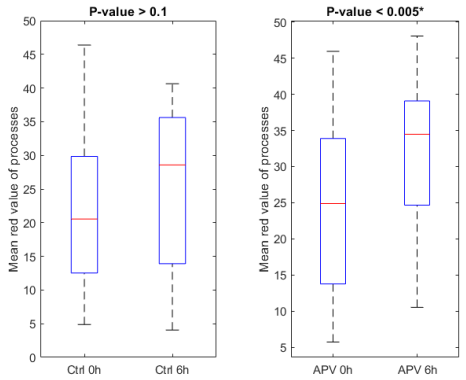

Figure 8: Comparison of control and APV conditions (N = 40). All images are taken as individual data points. The Wilcoxon rank sum test was used to compare each condition to each other with the resulting P-values: between controls and APV, 0.1029 and 0.0021 respectively.

A difference in control per experiment was also analysed. This can be seen in Figure 10. For the controls, no difference can be found in each independent experiment (all p-values higher than 0.15), although experiment 1 has higher values then 2 and 3.

Finally, for all different puncta thresholds, no significant differences were found between APV 0h and APV 6h (all p-values higher than 0.4).

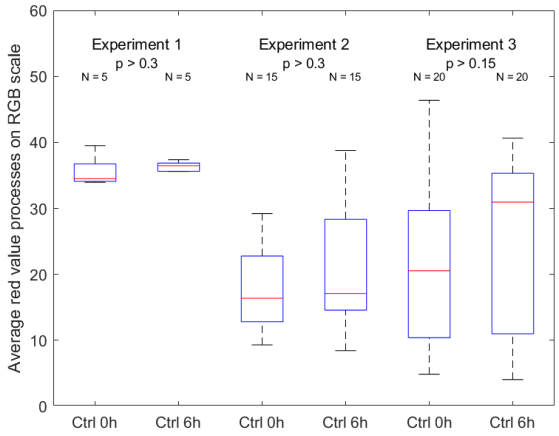

Figure 10: Control conditions in comparison with experiment batches, also showing amount of images in each experiment. The p-values were determined by the Wilcoxon rank sum test. No significant differences between ctrl 0h and 6h per experiment were found. Experiment 1 did have higher values in general.

Therefore, no further analysis was done with the puncta threshold data. An overview of these datasets can be found in Figure 9. The higher the threshold, the lower the percentage. The exact values for each condition for mean red intensity and the different puncta thresholds can be found in Appendix B.

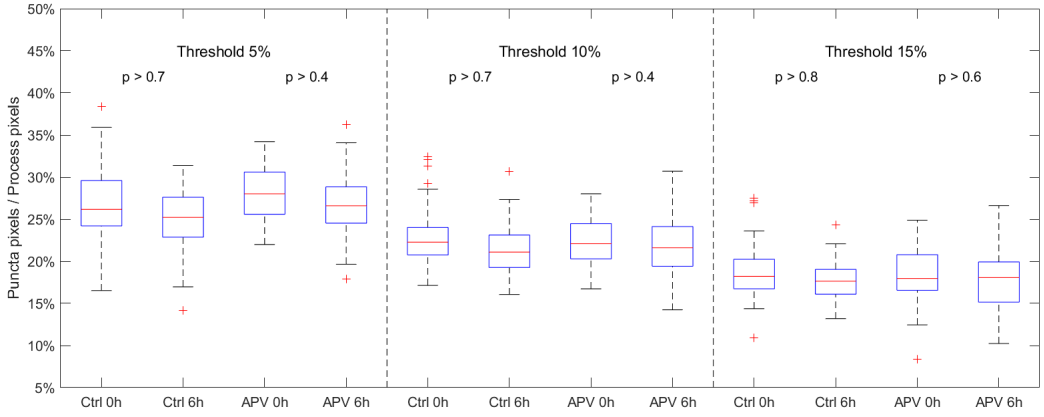

Figure 9: Boxplot of all results for the different puncta thresholds (for each condition N = 40). An average was computed for each local area. Since puncta are slightly brighter than their surroundings, they will exceed this average. Thresholds were set up for these values, being: 5%, 10% and 15% above the local found average. No significant differences were found in all comparisons between control groups and between APV groups.

4 Discussion

A significant difference was found between APV 0h and APV 6h for the mean red intensity. It was generally higher, which could mean AMPA tries to compensate for NMDA blockers by increasing the amount of AMPA receptors in existing synapses. No significant increases were found in all thresholds for puncta. This could indicate that no silent synapses are unsilenced by AMPA receptors after NMDA blockage.

A mechanism that could explain the AMPA receptors increase is one that G. Turrigiano describes as synaptic scaling. In synaptic scaling, neurons adapt their firing rate back to normal after a disturbance. She mentions the following pathway: a decrease in firing rate leads to a decrease in Ca^{2+}-ions. This reduces the activity of CaMKIV that eventually leads to increased accumulation of AMPA receptors. Ca^{2+} increases again, starting a negative feedback loop[15]. Since NMDA receptors are an important source of Ca^{2+}, Ca^{2+} would decrease after blockage through APV[9]. This could also start the pathway described by G. Turrigiano, leading to an increase in accumulation of AMPA receptors. Silent synapses are left out in this explanation, yet that may be due to a different mechanism. D. Liao found that activation of NMDA receptors in silent synapses by spontaneous synaptic activity results in rapid recruitment of AMPA receptors[16]. So, to unsilence these synapses with AMPA receptors could need specific NMDA input, that is inaccessible when NMDA is blocked.

Not all images were taken simultaneously. The first images were made separately in 2023, while 2 and 3 were made with the same configurations in 2024. Two different observers took the photos. The protocols differed in waiting time after addition of blocking buffer, where experiment 2 and 3 would wait 1-1.5 hours longer.

The incubation time was another difference between experiments. Experiment 3 had a week less in the incubator, this was done by mistake. During the experiments, the shorter time in incubator was not noticed. Only afterwards the oversight became apparent.

Finally, as previously said, DAPI was used to search for locations, which sometimes failed due to the chosen image being too red to successfully apply eroding. This would lead to the image taken based on AMPA staining. This should be avoided at all cost in the next experiment; no photos should be taken based on the readout. Another effect of using DAPI to take pictures, was that most images were taken on the outside of the coverslip, which occasionally had different morphology. In general, the middle of each coverslip had a larger amount of red and cells, which made analysis difficult. If the script were changed to differentiate processes more from unfocused or crowded areas, these locations would be more accurate to analyse, instead of the outer edges. The outer edges can provide astrocytes space to divide, which can influence the images, since only neurons have to be looked at. Another advantage to improving the script would be to include more consistency, because the morphology changed from time to time, see figure 12 in Appendix C.

Another aspect that needs to be mentioned is the two-step or indirect immunostaining. For direct immunostaining, the ratio between signal and receptors is one on one; one antibody binds to one receptor only. More fluorescence means more target sites. For two-step immunostaining, the secondary antibody can bind multiple times to the same primary antibody. The ratio can vary, but the assumption was that more fluorescence showed more AMPA receptors. Indirect immunostaining was chosen to improve image quality and analysis, since it provides more signal than direct immunostaining.

Some improvements can be made regarding the script. While good at detecting subtle processes, it fails when it needs to select obvious ones. This is often occurring in images with high amounts of red intensity. Since the code looks at all the red in total before eroding, it does not differ between shades of red. After eroding a very red image, it selects only the parts around a black area in the original image. A solution to this could be apart from eroding the pixels, performing edge detection: first the normal check of red threshold will be done. If the area is too large, another check will be done looking at differences in intensity, thus checking edges. This will likely result in another problem; what is the beginning, body or end of that process, which has to be

determined through having a higher intensity. This approach was not implemented due to the thought occurring in later stages of the project, but can be used in a follow-up script. For an image containing much red in the current script, see Appendix A.

Using the DAPI images as cell body detectors can be another way of analysing the images. DAPI stains nuclei blue, with a black background. This could create a mask of where not to analyse, helping the eroding step. Nonetheless, this cannot account for different cell body shapes, which the eroding step does attempt to achieve.

Finally, the puncta detecting also needs to be improved in future projects. Due to time constraints, the current method has not been tested extensively enough. It could be too sensitive for false-negatives or mistake false-positives. This should be further revised in upcoming projects. Instead of looking at one entire area, it can be divided into more local parts to accurately present the local average, thus brighter points.

5 Conclusion

After blockage of NMDA receptors with APV, a significant difference was found in fluorescence intensity that implies an increase in AMPA receptors. This answers the research question and could explain why there is a peak at 6 hours for electrical stimulation response in cortical rat cells in Figure 2. Through what mechanism this is achieved, needs to be researched in a different experiment. Furthermore, no difference in new puncta was found, though this needs to be investigated more thoroughly.

6 Acknowledgements

The making of this article could not have been possible without the guidance, feedback and supervision from Dr. Ir. J. Le Feber and Martina Lamberti. I want to thank Gerco Hassink and Marloes Levers as well for helping with the lab experiments and setup of the microscope, and dr. S.U. Yavuz for providing even more feedback. Lastly, all friends who in some way also gave input or feedback, have my thanks.

References

1. P. E. Ludwig, V. Reddy, M. Varacallo, *StatPearls* **2023**.
2. M. J. Caire, V. Reddy, M. Varacallo, *StatPearls* **2023**.
3. Y. Zhou, N. C. Danbolt, *Journal of Neural Transmission* **2014**, *121*, 799.
4. B. E. Jewett, B. Thapa, *StatPearls* **2022**.
5. M. W. Sherwood, S. H. Oliet, A. Panatier, *International Journal of Molecular Sciences* **2021**, *22*, DOI 10.3390/IJMS22147258.
6. D. Purves, G. J. Augustine, D. Fitzpatrick, W. C. Hall, A.-S. LaMantia, L. E. White, *Neuroscience*, 5th, (Eds.: R. D. Mooney, M. L. Platt), Sinauer Associates, Inc., Massachusetts, **2012**.
7. T. V. Bliss, S. F. Cooke, *Clinics* **2011**, *66*, 3.
8. D. E. Feldman, *Neuron* **2012**, *75*, 556–571.
9. Y. Inglebert, D. Debanne, *Frontiers in Cellular Neuroscience* **2021**, *15*, 727336.
10. M. Lamberti, M. J. v. Putten, S. Marzen, J. l. Feber, *bioRxiv* **2024**, 2024.02.01.578348.
11. D. M. Kullmann, S. A. Siegelbaum, *Neuron* **1995**, *15*, 997–1002.
12. Research — The Klein Lab.
13. Pipette - Free healthcare and medical icons.
14. File:202012 Cell culture plate size 24 wells.svg - Wikimedia Commons.
15. G. G. Turrigiano, *Cell* **2008**, *135*, 422–435.
16. D. Liao, R. H. Scannevin, R. Huganir, *The Journal of Neuroscience* **2001**, *21*, 6008.

A Analysis of an image containing much fluorescence

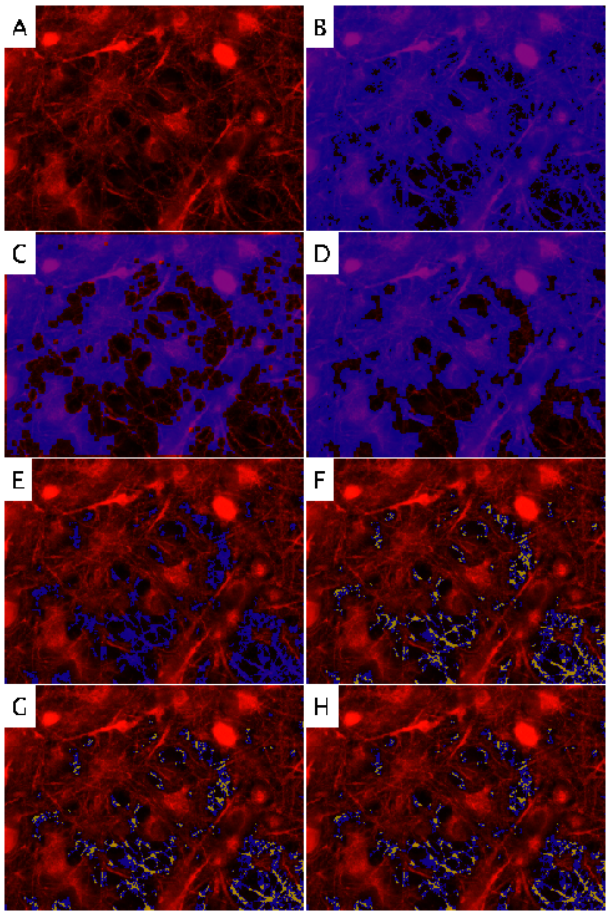

Figure 11: Another example of the step-by-step analysis done by MATLAB. A: original image with red immunostaining of AMPA at 60x magnification. All other images have an overlay of this image. B: all red values above 10% of the maximum red value, shown in blue. C: parts remaining after eroding B. D: parts after enlarging C (see text). E: resulting parts after excluding D from B. F-G: blue is the selected processes of E, with yellow being pixels above the set thresholds of the local average of 5% (F), 10% (G) and 15% (H)

For this image, the script does not distinguish different shades of red. Every pixel that is above the 10% of max red value is selected in B, then eroding etc. is applied. Processes that are surrounded by red are not sufficiently selected through this method for these types of images. This could be solved by using intensity as eroding factor, rather than pixels. However, this needs to be tested in future scripts.

B Table with medians and IQR of all data

Table 1: All values for the medians and interquartile ranges of all conditions. Mean red intensity is calculated for the selected processes. The thresholds for puncta are 5%, 10% and 15% above the local area average (see article).

All experiments		Control: Median (IQR)	APV: Median (IQR)
Mean red intensity	0h	20.55 (17.33)	24.88 (20.12)
	6h	28.58 (21.70)	34.47 (14.42)
Puncta threshold 5%	0h	26.17 (5.38)	28.02 (5.01)
	6h	25.22 (4.74)	26.60 (4.31)
Puncta threshold 10%	0h	22.28 (3.26)	22.10 (4.19)
	6h	21.10 (3.86)	21.61 (4.72)
Puncta threshold 15%	0h	18.22 (3.51)	17.97 (4.23)
	6h	17.64 (2.94)	18.07 (4.78)

C Different images of the same coverslip

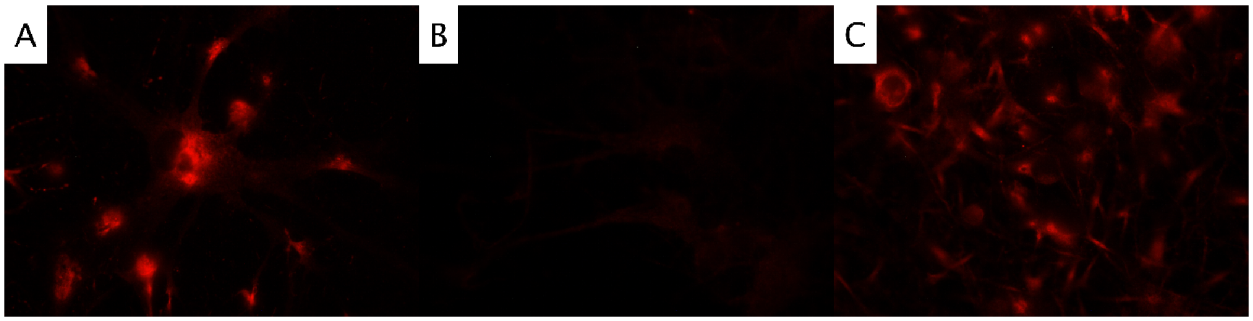

Figure 12: All these images were taken in the same coverslip. Only A and B were analysed, C was taken for the shape of the cells.

Dutch summary

Eerder onderzoek toonde een onverwachte toename in elektrische stimulatieactiviteit zes uur na toevoeging van APV aan bij corticale rattencellen in vitro. Omdat een afname verwacht werd, werd het experiment herhaald met immunokleuring. Fluorescente foto's van neuronale uitlopers op nul en zes uur werden geanalyseerd om te kijken of de totale hoeveelheid AMPA-receptoren veranderde en of de hoeveelheid synapsen toenam. De analyse omvatte de kleurintensiteit van de uitlopers en puncta. Uiteindelijk werd er een verschil gevonden in de gemiddelde kleurintensiteit van de uitlopers, wat suggereert dat er meer AMPA-receptoren aanwezig zijn na de blokkering van NMDA-receptoren.